BILATERAL PARALLEL FORCE/POSITION TELEOPERATION CONTROL

Keyvan Hashtrudi-Zaad and **Septimiu E. Salcudean**
Department of Electrical and Computer Engineering
University of British Columbia
Vancouver, B.C., Canada V6T 1Z4
keyvanh@ece.ubc.ca , tims@ece.ubc.ca

ABSTRACT

The application of parallel force/position control to teleoperation systems is considered in this paper. Higher priority is given to position control at the master side and to force control at the slave side of the teleoperation system. The stability and performance of the proposed controller is investigated by analyzing the three decoupled systems obtained from projecting the closed-loop system dynamics onto the slave task-space orthogonal directions. Experimental results demonstrate the excellent force and position tracking performance provided by the new controller.

INTRODUCTION

Teleoperation systems are employed to enable humans to execute remote or dangerous tasks with enhanced safety, at lower cost, or even better accuracy. One of the major objectives in designing bilateral teleoperation control systems is achieving *transparency*, that is a match between the master and slave positions and forces.

In the past decade, a number of control architectures have been proposed to provide higher transparency performance (Salcudean, 1997), and only a few of those schemes have succeeded in offering perfect transparency under ideal conditions (Yokokohji and Yoshikawa, 1992),(Lawrence,1993). However, in practice due to the measurement noise, model uncertainties, and communication channel time-delays, the system performance is compromised and new mechanisms should be devised to provide enhanced force/position error regulation (Salcudean,1997).

As a simple solution, in this work, the idea of *parallel force/position control*, proposed in (Chiaverini and Sciavico, 1988,1992,1993,1994) for single robot compliant control is expanded and applied to teleoperation systems. In the application of parallel force/position control, higher priority is given to position control at the master side and to force control at the slave side.

This paper first reviews a simple version of parallel force/position control for a three degree-of-freedom (DOF) robot, and then discusses the system stability and steady-state performance on any type of LTI mass-damping-spring environment. Next, *bilateral parallel force/position teleoperation control* is introduced by applying parallel force/position control to a 3-DOF slave robot and the dual of that controller to a 3-DOF master robot. Following that, the spatial behavior of the operator-master pair is investigated using the geometrical tools provided earlier in the paper. Experimental results conducted on a single axis teleoperation system are presented next, and finally conclusions are drawn.

PARALLEL FORCE/POSITION CONTROL OF A SINGLE ROBOT

In this section, the contact geometry of a 3-DOF manipulator in contact with a plannar environment studied in (Chiaverini and Sciavico, 1988), and a simple linear version of parallel force/position control proposed in the same paper are reviewed. In addition, the stability of the controlled system considering a linear mass-damper-spring environment model is further analyzed. These provide the preliminary tools for the introduction and analysis of bilateral parallel force/position control for a 3-DOF teleoperation system to be presented in the next section.

Consider the end-effector of a 3-DOF manipulator in contact with a planar environment, as shown in Fig. 1. Assuming a linear mass model for the manipulator [1] and

[1] It is assumed that the nonlinear terms of the manipulator dynamics, if any, are cancelled out using inverse dynamics (Chiaverini and Sciavico, 1988).

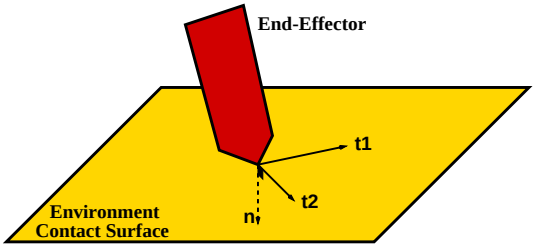

Figure 1. Robot end-effector in contact with a planar environment.

only translational motion for the end-effector, the dynamic equation for the coupled system can be written as

$$\mathbf{f_c} = \mathbf{M_r}\ddot{\mathbf{x}}_\mathbf{e} + \mathbf{f_e} \tag{1}$$

where $\mathbf{M_r}, \mathbf{x_e}, \mathbf{f_e}$ and $\mathbf{f_c}$ denote the robot mass matrix, the end-effector position, the environment contact force, and the control force command to the robot actuators, respectively [2]. Assuming negligible friction at the contact and neglecting the effect of contact local deformation due to the high rigidity of the environment (Chiaverini and Sciavico, 1988), the environment force $\mathbf{f_e}$ is always orthogonal to the plane and has no tangential component to the surface. Therefore, if an orthonormal task coordinate frame $\mathcal{C}_\mathcal{T}$ is defined with a unit basis vector $\mathbf{n}$ along the contact normal, and the other two basis vectors $\mathbf{t_1}$ and $\mathbf{t_2}$ tangent to the contact surface, the contact force and position can be represented as (Chiaverini and Sciavico, 1988)

$$\mathbf{f_e} = f_{e1}\mathbf{t_1} + f_{e2}\mathbf{t_2} + f_{en}\mathbf{n} = f_{en}\mathbf{n} \tag{2}$$

$$\mathbf{x_e} = x_{e1}\mathbf{t_1} + x_{e2}\mathbf{t_2} + x_{en}\mathbf{n} \ , \tag{3}$$

where x_{e1}, x_{e2} and $f_{e1} = f_{e2} = 0$ are the position and force components in the tangential directions, and x_{en} and f_{en} are the position and force components in the normal direction. Also, a linear mass-damper-spring model for the environment in the latter direction is assumed, that is

$$f_{en} = M_{en}\ddot{x}_{en} + B_{en}\dot{x}_{en} + K_{en}(x_{en} - x_{eon}) \ , \tag{4}$$

where x_{eon} is the resting point of the environment in the normal direction at which $f_{en} = 0$. In our case, it is assumed that the resting point is stationary, that is $\dot{x}_{eon} = 0$. From (2)-(4), one can show that

$$\mathbf{F_e} = \mathbf{Z_e}(\mathbf{X_e} - \mathbf{X_{eo}}) \ , \tag{5}$$

[2] In this paper, all matrices and vectors are in boldface letters, and all variables are expressed with respect to a fixed orthonormal Cartesian reference coordinate frame $\mathcal{C}_\mathcal{R}$.

where $\mathbf{F_e}, \mathbf{X_e}$ and $\mathbf{X_{eo}}$ are the Laplace transforms of $\mathbf{f_e}, \mathbf{x_e}$ and $\mathbf{x_{eo}}$, and $\mathbf{Z_e}$ is the environment impedance matrix defined as

$$\begin{aligned}\mathbf{Z_e} &:= ({}^\mathcal{R}\mathbf{R}_\mathcal{T})diag(0,0,Z_{en})({}^\mathcal{R}\mathbf{R}_\mathcal{T})^T \\ &= Z_{en}\mathbf{n}\mathbf{n}^T := (M_{en}s^2 + B_{en}s + K_{en})\mathbf{n}\mathbf{n}^T \ . \end{aligned} \tag{6}$$

Here, ${}^\mathcal{R}\mathbf{R}_\mathcal{T} = [\mathbf{t_1}\ \mathbf{t_2}\ \mathbf{n}]$ denotes the rotation matrix from $\mathcal{C}_\mathcal{T}$ to $\mathcal{C}_\mathcal{R}$, and the superscript ^{T} is the transpose operator.

In a general contact task, manipulators are expected to follow the force/position profile

$$\mathbf{f_{ed}} = f_{ed1}\mathbf{t_1} + f_{ed2}\mathbf{t_2} + f_{edn}\mathbf{n} \tag{7}$$

$$\mathbf{x_{ed}} = x_{ed1}\mathbf{t_1} + x_{ed2}\mathbf{t_2} + x_{edn}\mathbf{n} \ , \tag{8}$$

where if there is enough information about the environment, the planning is done so that $f_{ed1} = f_{ed2} = 0$ (Raibert and Craig, 1981). Unfortunately, due to the environment mechanical impedance properties, it is usually impossible for the end-effector to fulfill $x_{en} = x_{edn}$ and $f_{en} = f_{edn}$ simultaneously. Therefore, a compromise between contact position and force tracking is made (Chiaverini and Sciavico, 1988),(Hogan, 1985). Often, for the safety of the environment and manipulator, force tracking is given higher priority than position tracking, such as in *parallel force/position control* (Chiaverini and Sciavico, 1988, 1992, 1993, 1994). In general, the control methodology enjoys the simplicity of the *impedance control* and at the same time provides the force/position control benefit of the *hybrid control* in artificial/natural directions, while taking full advantage of all the measurements. An easy to implement linear version of this control strategy (Chiaverini and Sciavico, 1993, 1994) which is going to be used for teleoperation control purposes in the next section, consists of PD position and PI force control terms with control parameter matrices $\mathbf{K_p}, \mathbf{K_v}$ and $\mathbf{K_f}, \mathbf{K_i}$ given by

$$\begin{aligned}\mathbf{f_c} = \mathbf{M_r}\ddot{\mathbf{x}}_\mathbf{ed} &+ \mathbf{K_v}(\dot{\mathbf{x}}_\mathbf{ed} - \dot{\mathbf{x}}_\mathbf{e}) + \mathbf{K_p}(\mathbf{x_{ed}} - \mathbf{x_e}) \\ &+ \mathbf{K_f}(\mathbf{f_{ed}} - \mathbf{f_e}) + \mathbf{K_i}\int_0^t (\mathbf{f_{ed}} - \mathbf{f_e})d\tau + \mathbf{f_e} \ . \end{aligned} \tag{9}$$

Combining (1) and (9) yields the closed-loop dynamics

$$\begin{aligned}&\mathbf{M_r}(\ddot{\mathbf{x}}_\mathbf{e} - \ddot{\mathbf{x}}_\mathbf{ed}) + \mathbf{K_v}(\dot{\mathbf{x}}_\mathbf{e} - \dot{\mathbf{x}}_\mathbf{ed}) + \mathbf{K_p}(\mathbf{x_e} - \mathbf{x_{ed}}) + \\ &\mathbf{K_f}(\mathbf{f_e} - \mathbf{f_{ed}}) + \mathbf{K_i}\int_0^t (\mathbf{f_e} - \mathbf{f_{ed}})d\tau = 0 \ , \end{aligned} \tag{10}$$

or simply

$$(\mathbf{M_r}s^2 + \mathbf{K_v}s + \mathbf{K_p})(\mathbf{X_e} - \mathbf{X_{ed}}) + (\mathbf{K_f} + \frac{\mathbf{K_i}}{s})(\mathbf{F_e} - \mathbf{F_{ed}}) = 0 \tag{11}$$

in the s-plane domain, where $\mathbf{X_{ed}}$ and $\mathbf{F_{ed}}$ are the Laplace transforms of $\mathbf{x_{ed}}$ and $\mathbf{f_{ed}}$.

Assuming $\mathbf{M_r} = M_r\mathbf{I}_{3\times3}, M_r > 0$ (without loss of generality), and setting $\mathbf{K_v} = K_v\mathbf{I}_{3\times3}$, $\mathbf{K_p} = K_p\mathbf{I}_{3\times3}$, $\mathbf{K_f} = K_f\mathbf{I}_{3\times3}$, $\mathbf{K_i} = K_i\mathbf{I}_{3\times3}$, to add an isotropic behavior to the control law (10), the closed-loop dynamics (5)–(8) and (11) are decoupled and can be decomposed onto the task-space directions $\mathbf{t_1}, \mathbf{t_2}$ and $\mathbf{n}$ according to

$$(M_r s^2 + K_v s + K_p)X_{e1,2} = (M_r s^2 + K_v s + K_p)X_{ed1,2} + (K_f + \frac{K_i}{s})F_{ed1,2} \quad (12)$$

$$[(M_r + K_f M_{en})s^2 + (K_v + K_f B_{en} + K_i M_{en})s + (K_p + K_f K_e + K_i B_{en}) + \frac{K_i K_{en}}{s}]X_{en} = (M_r s^2 + K_v s + K_p)X_{edn} + (K_f + \frac{K_i}{s})F_{edn} + (K_f + \frac{K_i}{s})(M_{en}s^2 + B_{en}s + K_{en})X_{eon} \quad (13)$$

where $(\cdot_{1,2})$ notation is used to condense the system dynamics representation in $\mathbf{t_1}$ and $\mathbf{t_2}$ directions into one equation.

If the system is asymptotically stable, the desired force is constant, and the desired position in tangential directions is time-varying and in normal direction is constant, then in steady state

$$\bar{x}_{e1,2} = x_{ed1,2} + \frac{K_i}{K_p} f_{ed1,2} t \quad , \quad \bar{f}_{e1,2} = 0 \quad (14)$$

$$\bar{x}_{en} = x_{eon} + \frac{1}{K_{en}} f_{edn} \quad , \quad \bar{f}_{en} = f_{edn} \quad (15)$$

hold, where $\bar{(\cdot)}$ denotes the steady state value of the argument. If there is sufficient information about the system, then $f_{ed1,2} = 0$, and position tracking is satisfied in the tangential direction; otherwise, a drifting phenomenon happens at a rate depending on K_p and K_i. In the normal direction, the integral term on force gives its control a higher priority at the expense of position error (Chiaverini and Sciavico, 1993, 1994).

To achieve asymptotic stability [3], from the second-order system (12), the position control parameters K_v and K_p have to be positive, and from the third-order system (13), the force control parameters K_f and K_i have to satisfy $K_i K_{en} > 0,\ M_r + K_f M_{en} > 0,\ K_v + K_f B_{en} + K_i M_{en} > 0$ and

$$(K_v + K_f B_{en} + K_i M_{en})(K_p + K_f K_{en} + K_i B_{en}) > (M_r + K_f M_{en})K_i K_{en} \quad (16)$$

to render (13) Hurwitz. In most practical situations, the environment stiffness is dominant over damping and mass properties. Therefore, the stability condition comes down to the simple inequality

$$0 < M_r K_i K_{en} < K_v(K_p + K_f K_{en}) \quad (17)$$

by setting $B_{en} \approx 0$ and $M_{en} \approx 0$ in (16). Interestingly enough, even if the stiffness is not dominant, (16) can be rearranged as

$$[K_v K_i B_{en} + K_i M_{en}(K_p + K_i B_{en}) + K_f B_{en}(K_p + K_f K_{en} + K_i B_{en})] + [K_v(K_p + K_f K_{en}) - M_r K_i K_{en}] > 0 \quad (18)$$

implying that if $K_v, K_p, K_f, K_i > 0$, and (17) or

$$M_r K_i - K_v K_f < \frac{K_p K_v}{K_{en}} \ . \quad (19)$$

holds, then the closed-loop system is asymptotically stable. Condition (19) is satisfied for any environment stiffness value if

$$M_r K_i < K_v K_f \quad (20)$$

Therefore, for any robot modeled by the LTI system (1) and in contact with any environment modeled by the linear mass-damper-spring dynamics (5), parallel force/position control (9) is asymptotically stable provided that all the control parameters are positive and (20) is satisfied. This shows that to guarantee stability when operating on *unknown environments*, a minimum amount of velocity and force feedback are necessary. If the dynamic range of the environment stiffness is known apriori, then the above minima can be reduced by employing sufficient position feedback.

In the next section, the parallel force/position strategy is employed in a bilateral teleoperation control system, and the analysis tools provided in this section will be used to investigate the system performance and stability.

BILATERAL PARALLEL FORCE/POSITION CONTROL

Consider a teleoperation system with two 3-DOF master and slave manipulators modeled by linear mass dynamics as

$$\mathbf{f_{mc}} = \mathbf{M_m}\ddot{\mathbf{x}}_\mathbf{h} - \mathbf{f_h} \quad (21)$$

$$\mathbf{f_{sc}} = \mathbf{M_s}\ddot{\mathbf{x}}_\mathbf{e} + \mathbf{f_e} \quad (22)$$

[3] In (Chiaverini and Sciavico, 1993), the stability analysis has only been conducted for environments modeled by a linear spring.

where $\mathbf{x_h}, \mathbf{x_e}, \mathbf{f_h}, \mathbf{f_e}, \mathbf{f_{mc}}$ and $\mathbf{f_{sc}}$ are vectors of the master and slave translational positions, force exerted by the operator on the master, force applied on the environment by the slave and the master and slave actuating control commands, respectively.

Assuming the same environment as used for the single robot in the previous section, and defining the same task-space coordinate frame $\mathcal{C}_\mathcal{T}$, (2)-(6) can be employed to represent the interaction dynamics between the slave and the environment, with $\mathbf{M_r} = \mathbf{M_s}$. However, unlike the slave-environment contact, since the operator grasps the master hand-controller, she/he can apply forces in every direction, and therefore the operator dynamics follows

$$\mathbf{F_h} = \mathbf{F_h^\star} - \mathbf{Z_h}\mathbf{X_h} \ , \tag{23}$$

where $\mathbf{X_h}, \mathbf{F_h}$ and $\mathbf{F_h^\star}$ are the Laplace transforms of $\mathbf{x_h}, \mathbf{f_h}$ and the operator's exogenous input force $\mathbf{f_h^\star}$, respectively, and $\mathbf{Z_h}$ denotes the operator's arm impedance matrix defined as

$$\begin{aligned}\mathbf{Z_h} &:= ({}^{\mathcal{R}}\mathbf{R}_\mathcal{T})diag(Z_{h1}, Z_{h2}, Z_{hn})({}^{\mathcal{R}}\mathbf{R}_\mathcal{T})^T \\ &= Z_{h1}\mathbf{t_1}\mathbf{t_1^T} + Z_{h2}\mathbf{t_2}\mathbf{t_2^T} + Z_{hn}\mathbf{n}\mathbf{n}^T \ .\end{aligned} \tag{24}$$

Here, it is assumed that the operator's arm dynamics can be adequately modeled by $Z_{h1,2} := M_{h1,2}s^2 + B_{h1,2}s + K_{h1,2}$ and $Z_{hn} := M_{hn}s^2 + B_{hn}s + K_{hn}$ in the three normal slave task-space directions $\mathbf{t_1}, \mathbf{t_2}$ and $\mathbf{n}$. Therefore, (23) can be decomposed into

$$F_{h1,2} = F^\star_{h1,2} - (M_{h1,2}s^2 + B_{h1,2}s + K_{h1,2})X_{h1,2} \tag{25}$$

$$F_{hn} = F^\star_{hn} - (M_{hn}s^2 + B_{hn}s + K_{hn})X_{hn} \ , \tag{26}$$

where

$$\mathbf{X_h} := X_{h1}\mathbf{t_1} + X_{h2}\mathbf{t_2} + X_{hn}\mathbf{n} \tag{27}$$

$$\mathbf{F_h} := F_{h1}\mathbf{t_1} + F_{h2}\mathbf{t_2} + F_{hn}\mathbf{n} \tag{28}$$

$$\mathbf{F_h^\star} := F^\star_{h1}\mathbf{t_1} + F^\star_{h2}\mathbf{t_2} + F^\star_{hn}\mathbf{n} \ . \tag{29}$$

To implement parallel force/position control at both the master and slave sides, intuitively, one should give higher priority to force control rather than position control at the slave side. This is because the level of information known from the slave side is much less than that from the master side, and in most of the applications the environment has to be protected from excessive contact forces. In addition, the slave force accommodation feature can be helpful in coping with the effects of unplanned collisions that result from the slave operating on unknown environments, especially when there are significant time-delays in the system and the slave momentarily operates in open-loop mode.

At the master side though, since the master is expected to mimic the environment impedance and the forces are matched by the slave controller, in a dual manner, higher priority has to be given to position control. Note that the force error integral term can also be added to the master controller; however, this brings no advantage as force error regulation is already obtained at the slave side. Setting $\mathbf{x_{ed}} = \mathbf{x_h}, \mathbf{x_{hd}} = \mathbf{x_e}, \mathbf{f_{ed}} = \mathbf{f_h}$ and $\mathbf{f_{hd}} = \mathbf{f_e}$, the bilateral parallel force/position control laws

$$\begin{aligned}\mathbf{f_{mc}} &= \mathbf{M_m}\ddot{\mathbf{x}}_\mathbf{e} + \mathbf{K_{xvm}}(\dot{\mathbf{x}}_\mathbf{e} - \dot{\mathbf{x}}_\mathbf{h}) + \mathbf{K_{xpm}}(\mathbf{x_e} - \mathbf{x_h}) \\ &\quad + \mathbf{K_{xim}}\int_0^t (\mathbf{x_e} - \mathbf{x_h})d\tau - \mathbf{K_{fpm}}(\mathbf{f_e} - \mathbf{f_h}) - \mathbf{f_h}\end{aligned} \tag{30}$$

$$\begin{aligned}\mathbf{f_{sc}} &= \mathbf{M_s}\ddot{\mathbf{x}}_\mathbf{h} + \mathbf{K_{xvs}}(\dot{\mathbf{x}}_\mathbf{h} - \dot{\mathbf{x}}_\mathbf{e}) + \mathbf{K_{xps}}(\mathbf{x_h} - \mathbf{x_e}) \\ &\quad + \mathbf{K_{fps}}(\mathbf{f_h} - \mathbf{f_e}) + \mathbf{K_{fis}}\int_0^t (\mathbf{f_h} - \mathbf{f_e})d\tau + \mathbf{f_e}\end{aligned} \tag{31}$$

are proposed where $\mathbf{K_{xvm}} = K_{xvm}\mathbf{I_{3\times 3}}$, $\mathbf{K_{xpm}} = K_{xpm}\mathbf{I_{3\times 3}}$, $\mathbf{K_{xim}} = K_{xim}\mathbf{I_{3\times 3}}$, $\mathbf{K_{fpm}} = K_{fpm}\mathbf{I_{3\times 3}}$, $\mathbf{K_{xvs}} = K_{xvs}\mathbf{I_{3\times 3}}$, $\mathbf{K_{xps}} = K_{xps}\mathbf{I_{3\times 3}}$, $\mathbf{K_{fps}} = K_{fps}\mathbf{I_{3\times 3}}$, and $\mathbf{K_{fis}} = K_{fis}\mathbf{I_{3\times 3}}$ are the master and slave position and force control matrices, and without loss of generality it is assumed that $\mathbf{M_m} = M_m\mathbf{I_{3\times 3}}, M_m > 0$, and $\mathbf{M_s} = M_s\mathbf{I_{3\times 3}}, M_s > 0$. Note that the scalar control gains are used to render the control law (30)-(31) isotropic. After eliminating $\mathbf{f_{mc}}$ and $\mathbf{f_{sc}}$ from (21)-(22) and (30)-(31), one obtains the dynamics of the closed-loop system as

$$\begin{aligned}&(\mathbf{M_m}s^2 + \mathbf{K_{xvm}}s + \mathbf{K_{xpm}} + \frac{\mathbf{K_{xim}}}{s})(\mathbf{X_h} - \mathbf{X_e}) = \\ &\qquad \mathbf{K_{fpm}}(\mathbf{F_h} - \mathbf{F_e})\end{aligned} \tag{32}$$

$$\begin{aligned}&(\mathbf{M_s}s^2 + \mathbf{K_{xvs}}s + \mathbf{K_{xps}})(\mathbf{X_h} - \mathbf{X_e}) = \\ &\qquad (\mathbf{K_{fps}} + \frac{\mathbf{K_{fis}}}{s})(\mathbf{F_e} - \mathbf{F_h}) \ .\end{aligned} \tag{33}$$

With the above choice of control matrices, the system degrees of freedom are decoupled and (32)-(33) can be easily decomposed along the three slave task-space directions $\mathbf{t_1}, \mathbf{t_2}$ and $\mathbf{n}$ using (2)-(4), (25)-(29) and $F_{e1,2} = 0$, according to

$$\begin{aligned}&[(M_m + K_{fpm}M_{h1,2})s^2 + (K_{xvm} + K_{fpm}B_{h1,2})s \\ &+(K_{xpm} + K_{fpm}K_{h1,2}) + \frac{K_{xim}}{s}]X_{h1,2} \\ &-(M_m s^2 + K_{xvm}s + K_{xpm} + \frac{K_{xim}}{s})X_{e1,2} = K_{fpm}F^\star_{h1,2}\end{aligned} \tag{34}$$

$$\begin{aligned}&[(M_m + K_{fpm}M_{hn})s^2 + (K_{xvm} + K_{fpm}B_{hn})s \\ &+(K_{xpm} + K_{fpm}K_{hn}) + \frac{K_{xim}}{s}]X_{hn} \\ &-[(M_m - K_{fpm}M_{en})s^2 + (K_{xvm} - K_{fpm}B_{en})s \\ &+(K_{xpm} - K_{fpm}K_{en}) + \frac{K_{xim}}{s}]X_{en} = K_{fpm}F^\star_{hn}\end{aligned} \tag{35}$$

for the master side, and

$$[(M_s - K_{fps}M_{h1,2})s^2 + (K_{xvs} - K_{fps}B_{h1,2} - K_{fis}M_{h1,2})s$$
$$+(K_{xps} - K_{fps}K_{h1,2} - K_{fis}B_{h1,2}) - \frac{K_{fis}K_{h1,2}}{s}]X_{h1,2}$$
$$-(M_s s^2 + K_{xvs}s + K_{xps})X_{e1,2} = \quad (36)$$
$$-(K_{fps} + \frac{K_{fis}}{s})F^{\star}_{h1,2}$$

$$[(M_s - K_{fps}M_{hn})s^2 + (K_{xvs} - K_{fps}B_{hn} - K_{fis}M_{hn})s$$
$$+(K_{xps} - K_{fps}K_{hn} - K_{fis}B_{hn}) - (\frac{K_{fis}K_{hn}}{s})]X_{hn}$$
$$-[(M_s + K_{fps}M_{en})s^2 + (K_{xvs} + K_{fps}B_{en} + K_{fis}M_{en})s$$
$$+(K_{xps} + K_{fps}K_{en} + K_{fis}B_{en}) + \frac{K_{fis}K_{en}}{s}]X_{en} =$$
$$-(K_{fps} + \frac{K_{fis}}{s})F^{\star}_{hn} \quad (37)$$

for the slave side. Unlike the single robot system described in the last section, the desired slave force command ($\mathbf{f_{ed}} = \mathbf{f_h}$) might have a component in the tangential direction. The reason is that the exogenous input force $\mathbf{f^{\star}_h}$ has components in all directions and the master hand-controller is capable of generating resisting forces in any direction, including $\mathbf{t_1}$ and $\mathbf{t_2}$. Assuming constant operator exogenous input, the steady-state analysis of (34)–(35) yields

$$\bar{x}_{h1,2} = \bar{x}_{e1,2} = \frac{f^{\star}_{h1,2}}{K_{h1,2}} \quad , \quad \bar{f}_{h1,2} = \bar{f}_{e1,2} = 0 \quad (38)$$

$$\bar{x}_{hn} = \bar{x}_{en} = \frac{f^{\star}_{h1,2}}{K_{hn} + K_{en}} \ , \ \bar{f}_{hn} = \bar{f}_{en} = \frac{K_{en}f^{\star}_{hn}}{K_{hn} + K_{en}} \ . \quad (39)$$

As it is seen from (38), although $f^{\star}_{h1,2} \neq 0$, unlike in (14), $\bar{x}_{h1,2}$ do not show any growing drift. This is because in this case $f_{e1,2} = 0$, and $x_{e1,2}$ acting as the master desired position commands are not exogenous and independent of the master dynamics. In fact, $\bar{x}_{h1,2} = \bar{x}_{e1,2}$ are adjusted in such a way that $f^{\star}_{h1,2}$ are absorbed in the operator's arm and consequently the master shows no resistance to the operator in the tangential directions, that is $\bar{f}_{h1,2} = 0$. The other issue is that all the position and force components match, whereas for a single robot only force error is regulated. This is because the master position and force that act as slave position and force commands embed the environment properties and are adjusted at the master side to comply with the environment force/position requirements.

To get better insight on position and force tracking, one can study the system transparency conditions. Consider the block diagram of a general four-channel architecture teleoperation control system as shown in Fig. 2, where $\mathbf{C_1}, ..., \mathbf{C_6}, \mathbf{C_m}, \mathbf{C_s}$ are rational transfer function control matrices, and $\mathbf{Z_m} = \mathbf{M_m}s^2, \mathbf{Z_s} = \mathbf{M_s}s^2, \mathbf{Z_h}$ and $\mathbf{Z_e}$ denote the master and slave system dynamics, operator

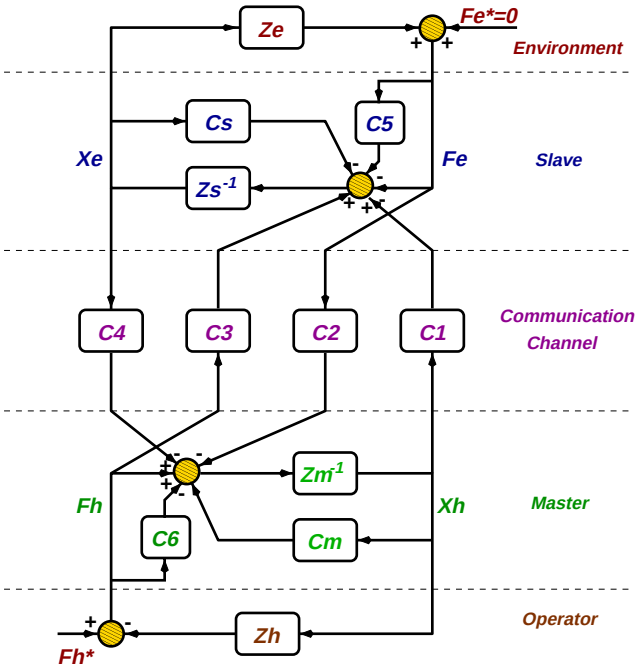

Figure 2. General block diagram of a four-channel teleoperation control system after Lawrence (1992), (Hashtrudi-Zaad and Salcudean, 1999).

impedance and slave impedance matrices, respectively. By comparing the system closed-loop dynamics (32)-(33) with the general system dynamic equations (Hashtrudi-Zaad and Salcudean, 1999)

$$(\mathbf{Z_m} + \mathbf{C_m})\mathbf{X_h} = (\mathbf{C_6} + \mathbf{I})\mathbf{F_h} - \mathbf{C_4}\mathbf{X_e} - \mathbf{C_2}\mathbf{F_e} \quad (40)$$
$$(\mathbf{Z_s} + \mathbf{C_s})\mathbf{X_e} = -(\mathbf{C_5} + \mathbf{I})\mathbf{F_e} + \mathbf{C_1}\mathbf{X_h} + \mathbf{C_3}\mathbf{F_h} \quad (41)$$

derived from Fig. 2, one reaches

$$\begin{cases} \mathbf{C_1} = \mathbf{Z_s} + \mathbf{C_s} \ = \ \mathbf{M_s}s^2 + \mathbf{K_{xvs}}s + \mathbf{K_{xps}} \\ \mathbf{C_2} = \mathbf{C_6} + \mathbf{I} \ = \ \mathbf{K_{fpm}} \\ \mathbf{C_3} = \mathbf{C_5} + \mathbf{I} \ = \ \mathbf{K_{fps}} + \frac{\mathbf{K_{fis}}}{s} \\ \mathbf{C_4} = -(\mathbf{Z_m} + \mathbf{C_m}) \\ \quad = -(\mathbf{M_m}s^2 + \mathbf{K_{xvm}}s + \mathbf{K_{xpm}} + \frac{\mathbf{K_{xim}}}{s}) \end{cases} , \quad (42)$$

which is the condition set for perfect transparency (Lawrence, 1993),(Hashtrudi-Zaad and Salcudean, 1999). Since the system is decoupled in all the three axes of $\mathcal{C}_{\mathcal{T}}$, a condition set similar to (42) also applies in each direction.

To analyze system stability, studying the stability of the sixth-order decoupled dynamics (34,36) and (35,37) is too involved. Instead, as shown in (Hashtrudi-Zaad and Salcudean, 1999), if the operator and environment are both passive, then the system stability is simplified to

$$\mathbf{C_2(Z_m + C_m) + C_3(Z_s + C_s) = 0} \tag{43}$$

being Hurwitz, or

$$\begin{aligned} &K_{fpm}s^2(M_s s^2 + K_{xvs}s + K_{xps}) + \\ &(K_{fps}s + K_{fis})(M_m s^3 + K_{xvm}s^2 + K_{xpm}s + K_{xim}) \\ &= (M_m K_{fps} + M_s K_{fpm})s^4 \\ &+(M_m K_{fis} + K_{xvm}K_{fps} + K_{xvs}K_{fpm})s^3 \\ &+(K_{xvm}K_{fis} + K_{xpm}K_{fps} + K_{xps}K_{fpm})s^2 \\ &+(K_{xpm}K_{fis} + K_{xim}K_{fps})s + (K_{xim}K_{fis}) = 0 \end{aligned} \tag{44, 45}$$

being Hurwitz. In the tangential directions where $f_{e1} = f_{e2} = 0$, or equivalently $K_{fpm} = 0$, or when the slave is not in contact, the characteristic equation (44) simplifies to the master and slave position control characteristic equations

$$M_m s^3 + K_{xvm}s^2 + K_{xpm}s + K_{xim} = 0 \tag{46}$$

$$M_s s^2 + K_{xvm}s + K_{xpm} = 0 \tag{47}$$

being stable and $K_{fps}, K_{fis} > 0$, which is easy to satisfy. In this way, one can use (46)-(47) and the desired free space transient performance to derive the position control parameters, and then find a feasible range of values for $(K_{fpm}, K_{fps}, K_{fis})$ to preserve stability by nonlinear programming starting from $(0, 1, 0)$.

It seems that by adding the integral terms, not only dynamic lag has been introduced in the closed-loop dynamics causing probable reduction in stability robustness, but also the system transparency has remained untouched as the perfect transparency conditions would still be satisfied if $K_{xim} = K_{fis} = 0$. However, in practice, as will be seen in the next section, a perfectly transparent system with no integral terms may show significant tracking errors, and the addition of the integral terms will reduce both the position and force errors drastically. The idea of parallel force/position can also be applied to non-transparent teleoperation systems to obtain virtually zero force and position errors. These will be demonstrated in the next section.

EXPERIMENTAL RESULTS

Figure 3 shows a photograph of the teleoperation experimental setup, consisting of two Maxon DC motors with handles acting as one-degree-of-freedom master (right) and slave (left) devices. The handles, equipped with JR^3 force sensors to measure operator and contact forces, are connected to the slave and master motors shafts through a 50:1 harmonic and a 10:1 single stage planetary gearhead, respectively. The motors are also equipped with position encoders. The sensors are connected to a VME-based computer system, consisting of data acquisition boards and a Sun SPARC 1e CPU board running the VxWorks real-time operating system. The system is networked to the local Ethernet and C programs are cross-compiled in the UNIX environment. The digital control loop is implemented at the sampling frequency $300(Hz)$.

Figure 3. Picture of the 1-DOF experimental setup.

After compensating for the master and slave Coulomb and viscous friction torques (Tafazoli et al., 1996), the SISO system dynamics can be expressed in terms of the motor scalar variables as in (21)-(22), where here f_{mc} and f_{sc} are the motor torque control commands, f_h and f_e denote the external torques applied by the operator on the master motor shaft and created by the slave motor shaft to be exerted on the environment, x_h and x_e are the master and slave motor shaft rotational positions, and finally $Z_m := I_m s, I_m = 3.35 \times 10^{-5}$ (Nms^2/rad) and $Z_s := I_s s, I_s = 3.00 \times 10^{-5} (Nms^2/rad)$ are the master and slave effective inertias, respectively. Note that the reason for using the motor variables is to have a pair of similar master and slave systems.

After closing the local feedback loops and feeding forward the position and torque information, the dynamic equations (40)–(42) are obtained where the position control transfer functions $C_m = 0.0034s + 0.1073 + \frac{1.0730}{s}$ and $C_s = 0.0024s + 0.0480$, are chosen to place the poles of the master and slave free motion dynamics (46)-(47) at -40, -40, -20 and -40, -40, respectively. Note that the velocity terms are derived from position measurements and no acceleration term is used, that is $C_1 = C_s$ and $C_4 = -C_m$. To find the force control parameters, using (44)-(45), a simple numerical search has been conducted in $K_{fpm}, K_{fps} \in (0, 2.0), K_{fis} \in (0, 4.0)$ range of force control parameters to check system stability. The search showed a stable system at all of these points, as long as the operator and environment are passive.

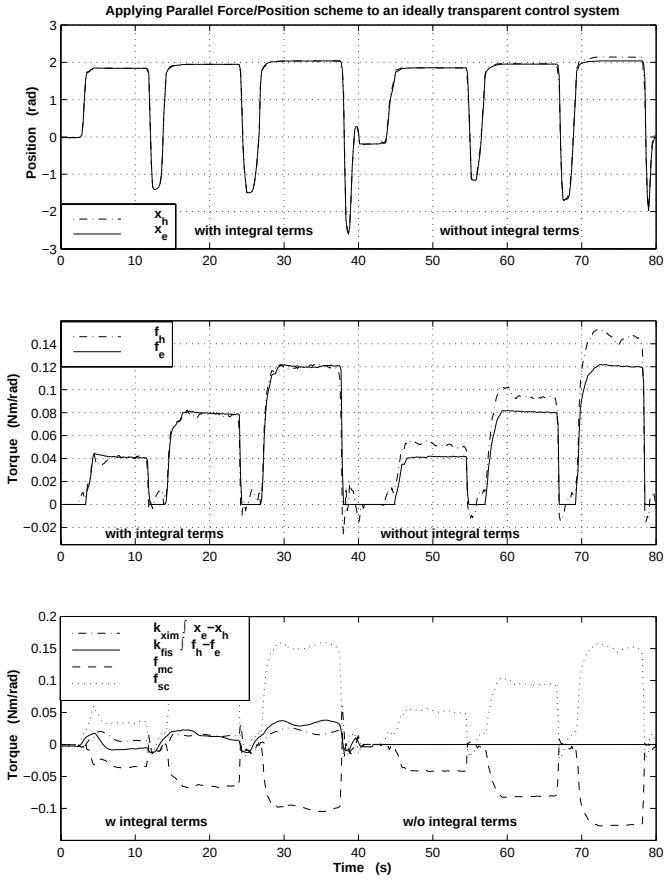

Figure 4. Application of the bilateral parallel force/position control to ideally transparent system ($C_2 = C_6 + 1.0 = 1.0$) reduces the force error significantly.

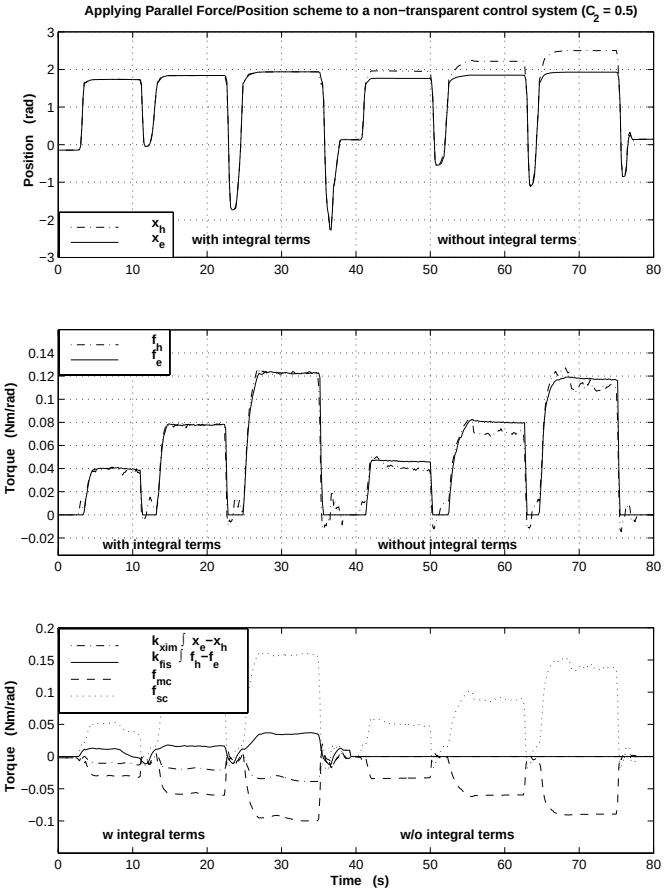

Figure 5. Application of the bilateral parallel force/position control to a non-transparent system ($C_2 = 0.5 \neq C_6 + 1.0 = 1.0$) reduces the position and force errors significantly.

The experiments conducted are categorized based on the control system ideal performance when the integral terms are not present in the control loop ($K_{xim} = K_{fis} = 0$) as follows: *i*) the control system is perfectly transparent with $C_2 = C_6 + 1 = 1.0$ and $C_3 = C_5 + 1 = 1.0$ (Lawrence, 1993), and *ii*) the system loses its transparency by reducing the slave force feedback by 50%, that is $C_2 = 0.5 \neq C_6 + 1.0 = 1.0$ and $C_3 = C_5 + 1 = 1.0$. In each experiment which lasts for 80 seconds, the operator pulls and pushes the master lever so that the slave makes six contacts with an environment of approximate stiffness $55,000(N/m)$ (or equivalently $K_{en} = 0.408(Nm/rad)$ if perceived from the slave motor) to maintain a desired contact torque at $0.4, 0.8$ or $1.2(Nm)$ level as shown in Figs. 4 and 5. For the first three contacts, parallel force/position control, *i.e.* addition of the integral terms, with $K_{xim} = 1.0730$ and $K_{fis} = 2.0$ are employed and in the following three the integral terms are removed for comparison.

As seen from the position and force profiles in Fig. 4, even for a system that is perfectly transparent in theory, due to the presence of noise, parametric and dynamic uncertainties, and time-delays, there is an average of 5% error in position tracking and a significant amount of 18% error in force tracking in contact regime (second set of three contacts). However, granting higher priority to position control at the master side and force control at the slave side have considerably reduced the average position and force tracking errors down to 0.03% and 0.2%, respectively (first set of three contacts). This positive effect is also easily visible in Fig. 5 for a non-transparent system.

If the integral coefficients K_{xim} and K_{fis} are chosen to be small and the slave is pushed into the contact for a long time, the integral of position and force errors may grow drastically. This may cause a resistive torque that keeps the slave pushing against the environment and the master resisting the operator's motion when she/he intends to pull

the master back. In other words, the unilateral environment constraint is transformed into a bilateral constraint. To solve this problem, the force/position error dynamics can be made faster by proper increase of the control coefficients. This results in smaller integrator windup. Also, one can pass the integral terms through a saturation filter to avoid integral windup effects. The control profiles in Figs. 4 and 5 clearly show the effect of the integral terms in the control efforts f_{mc} and f_{sc} in providing better tracking.

In conclusion, although bilateral parallel force/position approach may cause some phase lag in the control loop, the position and force tracking reduction is significant if the control parameters are properly chosen. The concept of higher priority for force control at the slave side and for position control at the master side can be implemented on any transparent (ideally) or non-transparent bilateral control system to obtain enhanced position and force tracking results. This strategy has been used by Anderson in (Anderson, 1990) to make the master desired force command and slave desired position command converge to the slave coordinating force command and the master position in steady state in the presence of time-delays.

CONCLUSIONS

The idea of parallel force/position control for a single robot has been tailored and extended to teleoperation systems by providing force control dominance at the slave side and position control dominance at the master side. For the first time, the system stability and performance have been investigated by decoupling and projecting the master-slave closed-loop system dynamics onto the slave task-space orthogonal directions. It has been shown that by proper selection of position and force control parameters, stability is maintained and the master faithfully mimics the environment in all directions in steady-state. The experimental results conducted on a single axis teleoperation system has shown significant enhancement in low speed position and force tracking. Future research will be directed towards the implementation of the bilateral parallel force/position control on multi-DOF teleoperation systems.

ACKNOWLEDGMENT

This work was supported by the Canadian IRIS/PRECARN Network of Centres of Excellence, Project IS-4. The authors wish to thank Wen–Hong Zhu for helping with the experimental setup.

REFERENCES

Anderson R.J., 1990, "Improved Tracking for Bilateral Teleoperation with Time Delay," *Robotics Research*, DSC-Vol. 26, pp. 233-239.

Chiaverini S., and Sciavicco L., 1988, "Force/Position Control of Manipulators in Task Space With Dominance in Force", *Proc. IFAC Robot Control*, pp. 137-143.

Chiaverini S., and Sciavicco L., 1992, "Edge-Following Strategies Using Parallel Control Formulation," *Proc. IEEE Int. Conf. Cont. Appl.*, pp. 31-36.

Chiaverini S., and Sciavicco L., 1993, "The Parallel Approach to Force/Position Control of Robotic Manipulators," *IEEE Trans. Rob. & Auto.*, Vol. 9, pp. 361-373.

Chiaverini S., and Sciavicco L., 1994, "Force/Position Regulation of Compliant Robot Manipulators," *IEEE Trans. Auto. Cont.*, Vol. 39, No. 3, pp. 647-652.

Hashtrudi-Zaad K., and Salcudean S.E., 1999, "On the Use of Local Force Feedback for Transparent Teleoperation," *Proc. IEEE Int. Conf. Rob. & Auto.*, pp. 1863-1869.

Hogan N., 1985, "Impedance Control: An Approach to Manipulation," Parts I-III, *Trans. ASME. J. Dyn. Syst. Meas., Cont.*, Vol. 107, pp. 1-24.

Lawrence D.A., 1992, "Designing Teleoperator Architectures for Transparency," *Proc. IEEE Int. Conf. Rob. & Auto.*, pp. 1406–1411.

Lawrence D.A., 1993, "Stability and Transparency in Bilateral Teleoperation," *IEEE Trans. Rob. & Auto.*, Vol. 9, No. 5, pp. 624-637.

Raibert M.H., and Craig J.J., 1981, "Hybrid Position/Force Control of Manipulators," *Trans. ASME J. Dyn. Syst. Meas., Cont.*, Vol. 103, pp. 126-133.

Salcudean S.E., 1997, "Control for Teleoperation and Haptic Interfaces", *Control Problems in Robotics and Automation*, B. Siciliano and K.P. Valavanis (Eds.), Springer-Verlag Lecture Notes in Control and Information Sciences, Vol. 230, pp. 50–66.

Tafazoli S., de Silva C.W., and Lawrence P.D., 1996, "Friction Modeling and Compensation in Tracking Control of an Electrohydraulic Manipulator," *Proc. IEEE Mediterranean Symp. New Dir. Cont. & Auto.*, pp. 375–380.

Yokokohji Y., and Yoshikawa T., 1992, "Bilateral Control of Master-slave Manipulators for Ideal Kinesthetic Coupling: Formulation and Experiment," *Proc. IEEE Int. Conf. Rob. & Auto.*, pp. 849–858.